Acta Cryst E CRYSTALLOGRAPHIC COMMUNICATIONS
ISSN 2056-9890

Crystal structure and Hirshfeld analysis of 3′-bromo-4-methylchalcone and 3′-cyano-4-methylchalcone

Zachary O. Battaglia,[a]‡ Jordan T. Kersten,[a]‡ Elise M. Nicol,[a]‡ Paloma Whitworth,[a]‡ Kraig A. Wheeler,[b] Charlie L. Hall,[c] Jason Potticary,[c] Victoria Hamilton,[c] Simon R. Hall,[c] Gemma D. D'Ambruoso,[a] Masaomi Matsumoto,[a] Stephen D. Warren[a] and Matthew E. Cremeens[a]*

[a]Department of Chemistry & Biochemistry, Gonzaga University, 502 E Boone Ave, Spokane, WA 99258, USA, [b]Department of Chemistry, Whitworth University, 300 W. Hawthorne Rd, Spokane, WA 99251, USA, and [c]School of Chemistry, University of Bristol, Cantock's Close, Bristol, BS8 1TS, England. *Correspondence e-mail: cremeens@gonzaga.edu

Received 21 July 2020
Accepted 13 August 2020

Edited by B. Therrien, University of Neuchâtel, Switzerland

‡ Authors contributed equally.

Keywords: crystal structure; chalcone; bromo; cyano; halogen bond; π stacking; edge-to-face.

CCDC references: 2023082; 2023081

Supporting information: this article has supporting information at journals.iucr.org/e

Two crystal structures of chalcones, or 1,3-diarylprop-2-en-1-ones, are presented; both contain a methyl substitution on the 3-Ring, but differ on the 1-Ring, bromo *versus* cyano. The compounds are 3′-bromo-4-methylchalcone [systematic name: 1-(2-bromophenyl)-3-(4-methylphenyl)prop-2-en-1-one], $C_{16}H_{13}BrO$, and 3′-cyano-4-methylchalcone {systematic name: 2-[3-(4-methylphenyl)prop-2-enoyl]benzonitrile}, $C_{17}H_{13}NO$. Both chalcones meaningfully add to the large dataset of chalcone structures. The crystal structure of 3′-cyano-4-methylchalcone exhibits close contacts with the cyano nitrogen that do not appear in previously reported disubstituted cyanochalcones, namely interactions between the cyano nitrogen atom and a ring hydrogen atom as well as a methyl hydrogen atom. The structure of 3′-bromo-4-methylchalcone exhibits a type I halogen bond, similar to that found in a previously reported structure for 4-bromo-3′-methylchalcone.

1. Chemical context

Chalcones are organic molecules commonly found in nature consisting of two phenyl rings connected by an α,β-unsaturated ketone, or enone. Interest in chalcone molecules has risen because of their potential pharmaceutical properties, electronic properties, and straightforward synthesis *via* a Claisen–Schmidt condensation between a benzaldehyde and acetophenone (Zhuang *et al.*, 2017). Pharmaceutical attributes shown by some chalcones include antioxidant, anti-inflammatory, anti-cancer, and cytotoxic properties (Sahu *et al.*, 2012). Additionally, some chalcones have been shown to be fluorescent, making them potential probes for mechanistic investigations and imaging (Lee *et al.*, 2012).

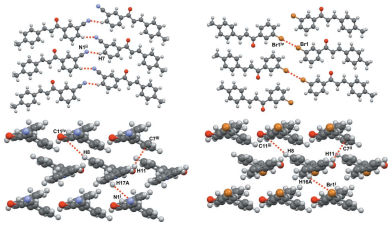

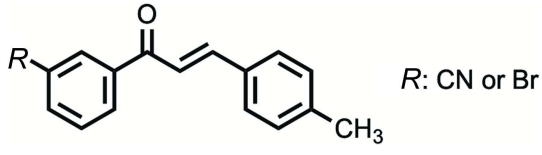

This paper compares the structure and packing of two newly crystallized chalcone molecules, 3′-cyano-4-methylchalcone [Sm6p] or *m*′CN*p*CH$_3$ and 3′-bromo-4-methylchalcone [Dm6p] or *m*′Br*p*CH$_3$, where Sm6p and Dm6p are internal codes tied to a large, long-term project. Each chalcone

OPEN ACCESS

Table 1
Selected angles (°).

The Φ1, Φ2, and Φ3 dihedrals are defined by C5—C4—C1—C2, C4—C1—C2—C3, and C2—C3—C10—C11, respectively.

Chalcone	Φ1	Φ2	Φ3	1-Ring 3-Ring Twist	1-Ring 3-Ring Fold
m′CN*p*CH$_3$	−154.58 (10)	−169.15 (10)	−163.34 (10)	49.11 (4)	0.67 (4)
m′Br*p*CH$_3$	−153.51 (16)	−169.73 (17)	−161.99 (18)	49.15 (6)	1.55 (6)

examined consists of a variable *meta* substitution at C6 of the 1-Ring, and methyl substitution at C13 of the 3-Ring, see Figs. 1 and 2. Substitution on the 1-Ring has been utilized to further understand the packing and structure of chalcone crystals based upon their ring substituents.

2. Structural commentary

The chalcones under observation, *m*′CN*p*CH$_3$ and *m*′Br*p*CH$_3$, differ at the *meta* position on the 1-Ring, cyano and bromo respectively, Figs. 1 and 2. Note that the following summary of dihedrals, which represents the planarity of the chalcones, references data in Table 1 where non-rounded angles and errors can be found. The enone core exhibits small (10–11°) deviations from planarity (Φ2) for *m*′CN*p*CH$_3$ and *m*′Br*p*CH$_3$. The 1-Ring/carbonyl twists (Φ1) show similar deviations from planarity (25–27°) for *m*′CN*p*CH$_3$ and *m*′Br*p*CH$_3$. The 3-Ring/alkene twists (Φ3) also show similar deviations from planarity (16–18°) for *m*′CN*p*CH$_3$ and *m*′Br*p*CH$_3$. *m*′CN*p*CH$_3$ and *m*′Br*p*CH$_3$ exhibit similar 1-Ring/3-Ring twist angles (approximately 49°) and fold angles (1–2°). Based on the angle values, *m*′CN*p*CH$_3$ and *m*′Br*p*CH$_3$ do not vary greatly in torsions despite their different substituents. Both chalcones are similarly twisted and show a pairwise antiparallel arrangement of the enone core (Fig. 3), which are related by inversion symmetry. A closer look at the supramolecular properties (see below) reveals similarities and differences for the crystal structures.

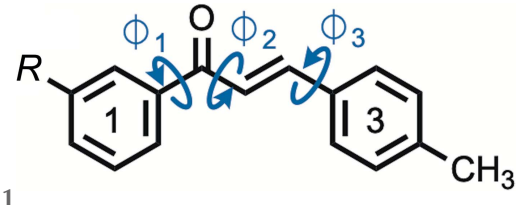

Figure 1
Three key dihedrals describing the chalcone planarity for 3′-cyano-4-methylchalcone (*m*′CN*p*CH$_3$) and 3′-bromo-4-methylchalcone (*m*′Br*p*CH$_3$); the 1-Ring and 3-Ring are labelled, where *R* = CN, Br.

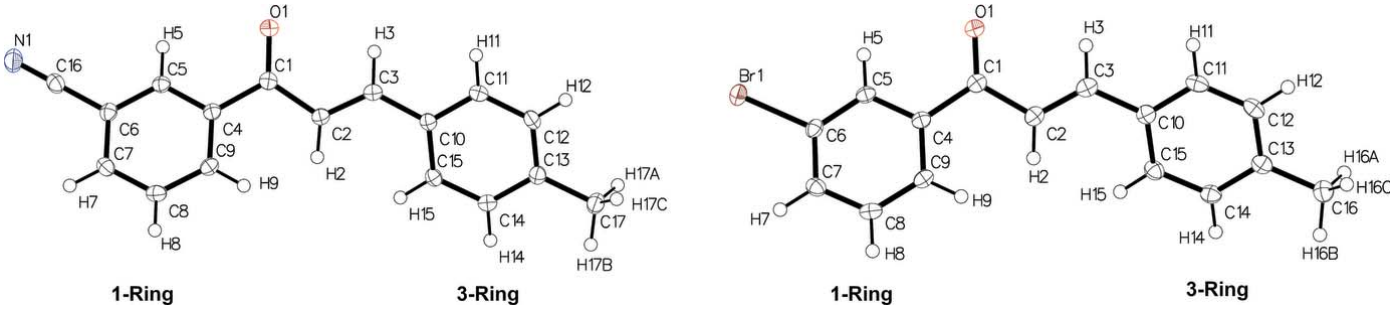

Figure 2
The asymmetric units of *m*′CN*p*CH$_3$ (left) and *m*′Br*p*CH$_3$ (right) showing the atom labeling with displacement ellipsoids drawn at the 50% probability level.

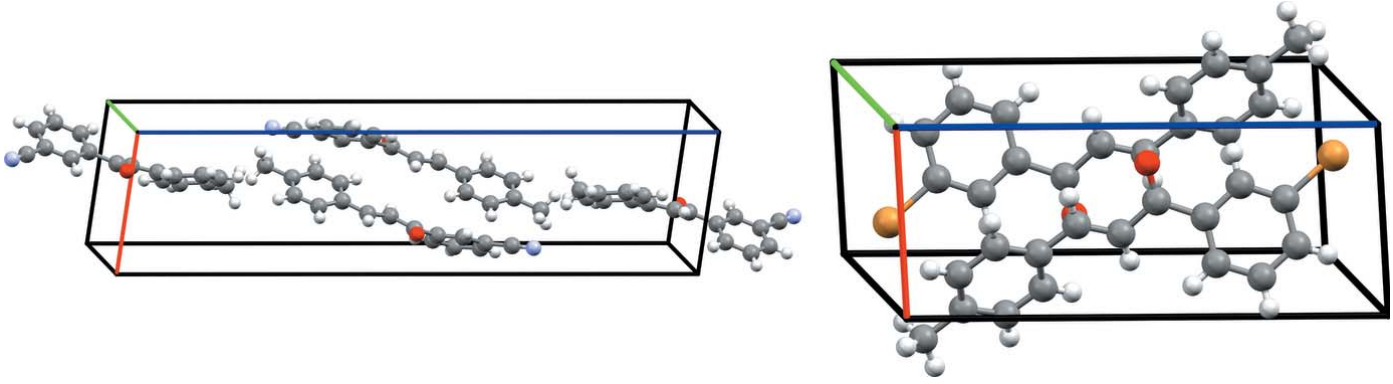

Figure 3
The unit cells of *m*′CN*p*CH$_3$ ($P2_1/c$ space group, left) and *m*′Br*p*CH$_3$ ($P\overline{1}$ space group, right), with the *a*, *b*, and *c* axes indicated in red, green, and blue, respectively.

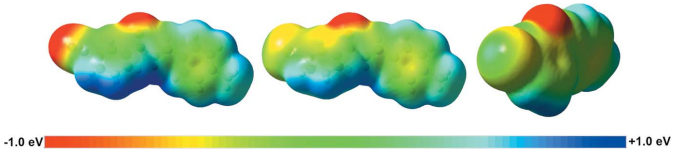

Figure 4
Electrostatic potentials at the wB97XD/6–311++G(d,p) level of theory for *m*′CN*p*CH$_3$ (left) and *m*′Br*p*CH$_3$ (middle and right). The range for all three plots is from −1.0 eV (red) to +1.0 eV (blue); electrostatic potential maps were plotted on the 0.0004 SCF density surface. Single point energy calculations were performed on the geometric coordinates of the asymmetric unit (Frisch *et al.*, 2009).

3. Supramolecular features

Electrostatic potentials are shown in Fig. 4, and Hirshfeld analyses are presented in Figs. 5–7 for *m*′CN*p*CH$_3$ and *m*′Br*p*CH$_3$. The electrostatic potentials show a greater polarization for *m*′CN*p*CH$_3$ than for *m*′Br*p*CH$_3$, which is expected because the cyano functional group is a stronger electron-withdrawing group than bromine. Consequently, the 1-Ring hydrogen atoms of *m*′CN*p*CH$_3$ exhibit greater partial positive character; nonetheless, the 1-Rings for both *m*′CN*p*CH$_3$ and *m*′Br*p*CH$_3$ show C—H$\cdots\pi$ interactions, see discussion below. Additionally, the small and slightly positive region on Br1 (Fig. 4, right) hints toward a σ-hole and an opportunity for a halogen bond in *m*′Br*p*CH$_3$. The Hirshfeld analyses below highlight the main intermolecular interactions found in *m*′CN*p*CH$_3$ and *m*′Br*p*CH$_3$ (Spackman & Jayatilaka, 2009); see the supporting information for fingerprint plots showing the percentage distribution of the intermolecular interactions represented by the d_{norm} surface in Fig. 5.

From a Hirshfeld analysis, the d_{norm} surfaces indicate close contacts (red regions) near H7, H8, H11, H17*A*, C7, C11, and N1 for *m*′CN*p*CH$_3$ and H8, C11, and Br1 for *m*′Br*p*CH$_3$. Upon closer inspection of these atoms, *m*′CN*p*CH$_3$ and *m*′Br*p*CH$_3$ contain multiple C—H$\cdots\pi$ interactions, which can be seen in Fig. 6 as red regions. Note that the following summary of short contacts between two atoms, which have distances less than the sum of their van der Waals (vdW) radii, references data found in Table 2 where non-rounded distances and errors can also be found. Notable hydrogen–carbon short contacts for *m*′CN*p*CH$_3$ are C8—H8$\cdots$C11^{iv} (2.88 Å) and C11—H11$\cdots$C7^{iii} (2.82 Å). In comparison, similar short contacts for

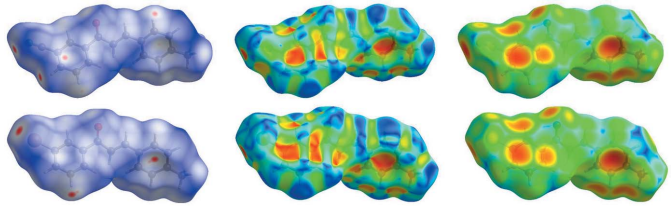

Figure 5
Hirshfeld surfaces of *m*′CN*p*CH$_3$ (top) and *m*′Br*p*CH$_3$ (bottom). Surfaces are mapped with d_{norm} (left), the shape-index (middle), and d_e (right). Note that close contacts involving the aromatic rings visualized in d_{norm} are also supported in both the shape-index and d_e, as indicated by the red regions over the rings.

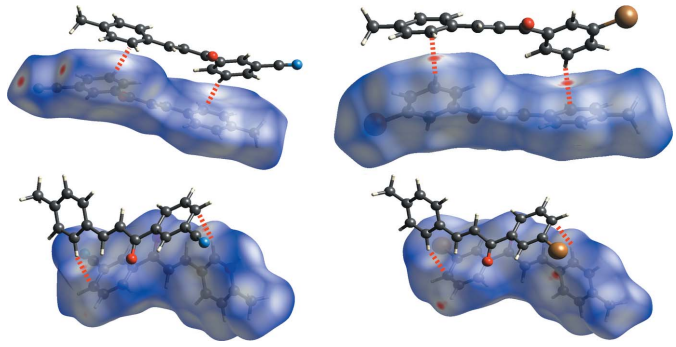

Figure 6
Hirshfeld short contact (d_{norm}) plots of *m*′CN*p*CH$_3$ (left) and *m*′Br*p*CH$_3$ (right) showing the C8—H8$\cdots$C11 (top) and C11—H11$\cdots$C7 (bottom) interactions. Red, white, and blue surface colors indicate contacts less than the sum of the van der Waals radii, close to, or greater than, respectively. For *m*′CN*p*CH$_3$ and *m*′Br*p*CH$_3$, the interacting chalcone molecules are antiparallel to one another with the carbonyl groups facing opposite each other.

m′Br*p*CH$_3$ are C8—H8$\cdots$C11^{iii} (2.80 Å) and C11—H11$\cdots$C7^{ii} (2.89 Å). *m*′CN*p*CH$_3$ contains some notable C—H$\cdots$N interactions, which can be seen in Fig. 7 as red regions. The hydrogen–nitrogen short contacts for *m*′CN*p*CH$_3$ are C7—H7$\cdots$N1^{ii} (2.60 Å) and C17—H17*A*$\cdots$N1^{i} (2.62 Å). For the sake of comparison to *m*′CN*p*CH$_3$, C7—H7$\cdots$Br1^{v} (3.24 Å) and C16—H16*A*$\cdots$Br1^{i} (3.10 Å) in *m*′Br*p*CH$_3$, which can be seen in Fig. 7 as white regions, have distances that are greater than the sum of bromine and hydrogen vdW radii (3.05 Å). Nonetheless, *m*′Br*p*CH$_3$ contains a Br$\cdots$Br interaction, see the red region associated with Br1 in Fig. 7. This type I halogen bond exhibits a short contact for Br1$\cdots$Br1^{iv} of 3.5565 (5) Å (Cavallo *et al.*, 2016).

For aromatic rings, π-stacking can exhibit multiple orientations, *e.g.* sandwich, parallel-displaced, and edge-to-face (Wheeler, 2011), arising largely from dispersion and/or electrostatic interactions. The C—H$\cdots\pi$ interactions of *m*′CN*p*CH$_3$ and *m*′Br*p*CH$_3$ resemble the edge-to-face orien-

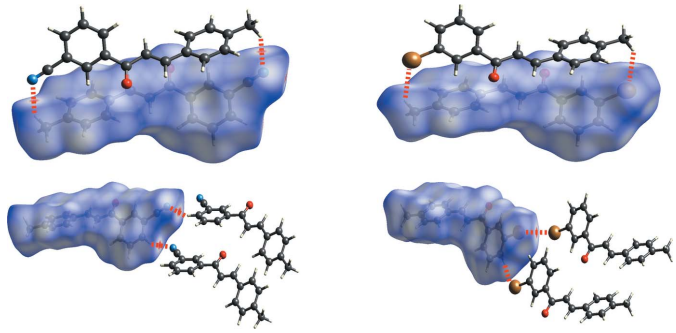

Figure 7
Hirshfeld short contact (d_{norm}) plots of *m*′CN*p*CH$_3$ (left) and *m*′Br*p*CH$_3$ (right) showing the C17—H17*A*$\cdots$N1 and C16—H16*A*$\cdots$Br1 (top), as well as C7—H7$\cdots$N1, C7—H7$\cdots$Br1, and C6—Br1$\cdots$Br1 (bottom) interactions. Red, white, and blue surface colors indicate contacts less than the sum of the van der Waals radii, equal to, or greater than, respectively. Note that the C7—H7$\cdots$N1 interaction for *m*′CN*p*CH$_3$ involves three molecules, while for *m*′Br*p*CH$_3$ both C7—H7$\cdots$Br1 and Br$\cdots$Br1 interactions are needed to support a similar three-molecule arrangement.

Table 2
Distances (Å) for close contacts.

Distances to the 1-Ring and 3-Ring reflect the distances to the centroids of those rings. The sums of the van der Waals radii (Å) for hydrogen plus carbon, nitrogen, or bromine are 2.9, 2.75, and 3.05, respectively, while the sum for bromine plus bromine is 3.7. The symmetry codes apply to those molecules interacting with the asymmetric unit. Estimated standard deviations are listed in parentheses.

m′CN*p*CH$_3$	Distance	*m*′Br*p*CH$_3$	Distance
C8—H8···C11^{iv}	2.8835 (11)	C8—H8···C11^{iii}	2.8019 (16)
C8—H8···3-Ring^{iv}	2.7391 (4)	C8—H8···3-Ring^{iii}	2.709 (2)
C11—H11···C7^{iii}	2.8187 (11)	C11—H11···C7^{ii}	2.8936 (17)
C11—H11···1-Ring^{iii}	2.8866 (4)	C11—H11···1-Ring^{ii}	3.061 (2)
1-Ring···3-Ring^{iv}	4.6036 (6)	1-Ring···3-Ring^{iii}	4.5176 (10)
3-Ring···1-Ring^{iii}	4.7132 (6)	3-Ring···1-Ring^{ii}	4.8989 (11)
C7—H7···N1^{ii}	2.5999 (9)	C7—H7···Br1^{v}	3.2379 (4)
C17—H17*A*···N1^{i}	2.6168 (11)	C16—H16*A*···Br1^{i}	3.0962 (3)
		Br1···Br1^{iv}	3.5556 (5)

Symmetry codes for *m*′CN*p*CH$_3$: (i) $1-x, 1-y, 1-z$; (ii) $-x, -\frac{1}{2}+y, \frac{1}{2}-z$; (iii) $-x, 1-y, 1-z$; (iv) $-x, -y, 1-z$. Symmetry codes for *m*′Br*p*CH$_3$: (i) $1-x, 1-y, 1-z$; (ii) $1-x, 2-y, 1-z$; (iii) $-x, 2-y, 1-z$; (iv) $2-x, 2-y, -z$; (v) $1-x, 2-y, -z$.

tation, which is also referred to as a T-shaped orientation. More specifically, the H8···3-Ring and H11···1-Ring interactions of *m*′CN*p*CH$_3$ and *m*′Br*p*CH$_3$ resemble a bent T-shaped orientation, or the so-called B-T1 orientation as defined by Dinadayalane & Leszczynski (2009). A computationally derived centroid-to-centroid distance for the B-T1 orientation is 4.63 Å (Dinadayalane & Leszczynski, 2009), which is close to the centroid distances for the 1-Ring···3-Ring^{iv} of *m*′CN*p*CH$_3$ (4.60 Å), the 1-Ring···3-Ring^{iii} of *m*′Br*p*CH$_3$ (4.52 Å), the 3-Ring···1-Ring^{iii} of *m*′CN*p*CH$_3$ (4.71 Å), and the 3-Ring···1-Ring^{ii} of *m*′Br*p*CH$_3$ (4.90 Å). See Table 2 for non-rounded distances and errors.

Inspection of packing diagrams indicate that the *m*′CN*p*CH$_3$ molecules form antiparallel sheets, Fig. 8. The interactions that contribute the most to this stacking are the C—H···π interactions (C8—H8···C11^{iv} or 1-Ring···3-Ring^{iv} and C11—H11···C7^{iii} or 3-Ring···1-Ring^{iii}) and C—H···N interactions (C17—H17*A*···N1^{i}), Figs. 6 and 7. All of these short contacts are less than their respective sum of vdW radii and are expected to contribute to the packing structure. Packing diagrams for *m*′Br*p*CH$_3$ also show antiparallel sheets, Fig. 8. Similar to *m*′CN*p*CH$_3$, the C—H···π interactions (C8—H8···C11^{iii} or 1-Ring···3-Ring^{iii} and C11—H11···C7^{ii} or 3-Ring···1-Ring^{ii}) are also contributors to this stacking arrangement. Both chalcones have strong interactions that contribute to the lateral arrangement of molecules in the packing diagrams. For *m*′CN*p*CH$_3$ this interaction is the C7—H7···N1^{i} interaction visualized in Fig. 7. For *m*′Br*p*CH$_3$, the Br1···Br1^{iv} interaction, or type 1 halogen bond, contributes to the lateral arrangement.

4. Database survey

A survey of the Cambridge Structural Database (CSD version 5.41, November 2019; Groom *et al.*, 2016), which excluded

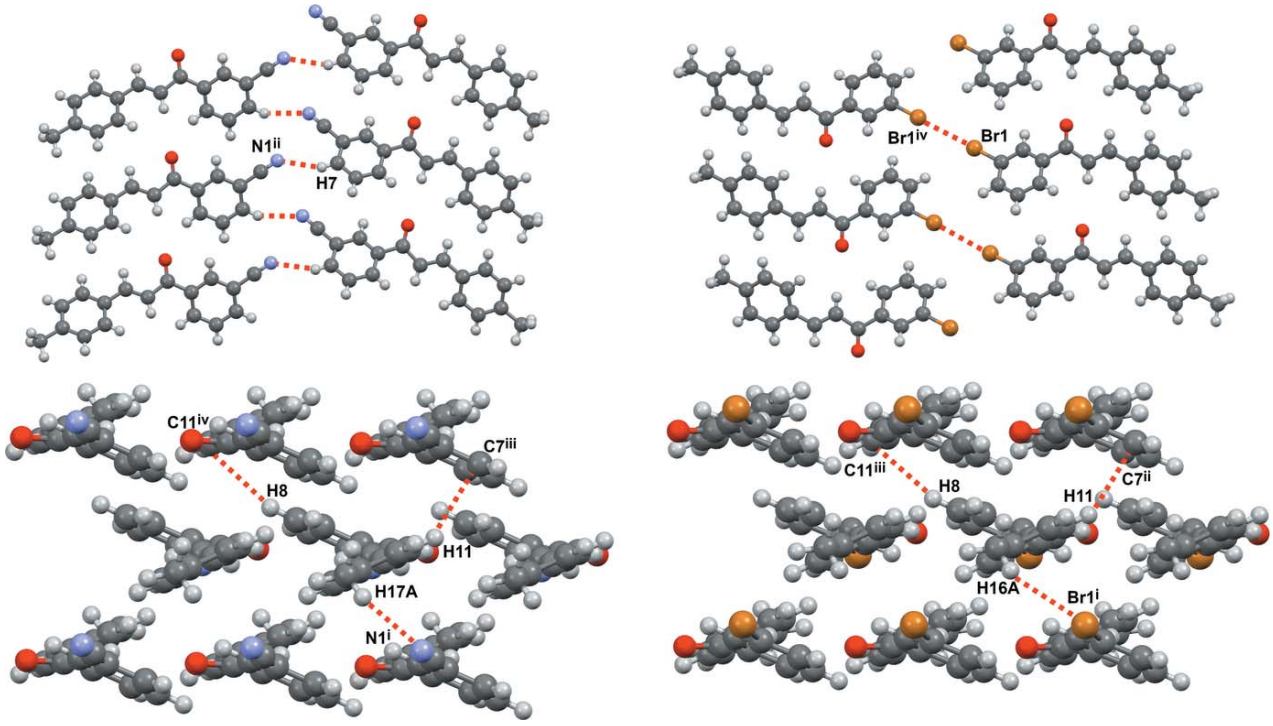

Figure 8
Selected packing displays for *m*′CN*p*CH$_3$ (left) and *m*′Br*p*CH$_3$ (right) showing identical lateral interactions for C16—N1···H7 and the Br1···Br1 type I halogen bond (top), as well as the stacking interactions N1···H17*A*, C11···H8, C7···H11, and Br1···H16*A* (bottom). The symmetry codes apply to those molecules interacting with the asymmetric unit. Additional N1···H7 and Br1···Br1 interactions are included to serve as a visual aid. Symmetry codes for *m*′CN*p*CH$_3$: (i) $1-x, 1-y, 1-z$; (ii) $-x, -\frac{1}{2}+y, \frac{1}{2}-z$; (iii) $-x, 1-y, 1-z$; (iv) $-x, -y, 1-z$. Symmetry codes for *m*′Br*p*CH$_3$: (i) $1-x, 1-y, 1-z$; (ii) $1-x, 2-y, 1-z$; (iii) $-x, 2-y, 1-z$; (iv) $2-x, 2-y, -z$.

chalcones substituted with additional rings, did not yield any mono-substituted cyanochalcone structures. The only disubstituted cyanochalcones found contained a *p*CN group on the 3-Ring; 4-cyano-2′-fluorochalcone [Bo19p] (LERXOW; $P\overline{1}$; Braun *et al.*, 2006*a*) and 4-cyano-4′-diethylaminochalcone [Qp19p] (NAWCEU; $P2_1/c$; Braun *et al.*, 2006*b*). Two of the CN structures, NAWCEU and *m*′CN*p*CH$_3$ [Sm6p], share the same space group, $P2_1/c$, while LERXOW belongs to the $P\overline{1}$ space group. *m*′CN*p*CH$_3$ is the first cyanochalcone crystal structure with a *meta*-cyano substituent and is the first disubstituted cyano-methyl-chalcone structure. Analysis of the close contacts for LERXOW and NAWCEU reveals different interactions than for *m*′CN*p*CH$_3$. Both structures display no strong interactions involving the cyano substituent, and instead both have strong interactions involving the carbonyl oxygen and the aromatic hydrogen atoms. LERXOW has a strong interaction between O1 and H3 and H11, while the oxygen interaction of note for NAWCEU is between O1 and H14. Additionally, C–H$\cdots\pi$ interactions have a lesser impact on the packing structure, as indicated by Hirshfeld analysis. More data are required to assess whether these differences are a function of *meta versus para* cyano substitution.

The same survey, again excluding molecules containing additional rings, showed multiple chalcones containing a bromo substitution, nine of which are substituted in the *meta* position of the 1-Ring, and two of which are disubstituted with a bromo and a methyl group. 3′-Bromochalcone [Dm-1] (CICLUW; $P\overline{1}$; Rosli *et al.*, 2007) and *m*′Br*p*CH$_3$ [Dm6p] belong to the same space group, $P\overline{1}$. The two disubstituted chalcones most similar to *m*′Br*p*CH$_3$, 4′-bromo-4-methylchalcone [Dp6p] (IZEFOI; $P2_1/c$; Wang *et al.*, 2004) and 3-bromo-4′-methylchalcone [Fp4m] (IGAPAI; $P\overline{1}$; Li *et al.*, 2008), are the only disubstituted Br/CH$_3$ chalcones. Of the two disubstituted chalcones, only IGAPAI shares the same space group as *m*′Br*p*CH$_3$, and IGAPAI also exhibits a type I halogen bond (Cavallo *et al.*, 2016), similar to *m*′Br*p*CH$_3$. IZEFOI does display C—H$\cdots\pi$ interactions, but these support a parallel arrangement, with the 3-Ring forming close contacts with the 3-Ring of a neighboring molecule, as opposed to the antiparallel nature of the C—H$\cdots\pi$ interactions for *m*′Br*p*CH$_3$. *m*′Br*p*CH$_3$ is the first methyl-substituted chalcone structure with an *m*′Br atom. Note that the codes Bo19p, Dm-1, Dm6p, Dp6p, Fp4m, Qp19p, and Sm6p are internal codes tied to a large, long-term project.

5. Synthesis and crystallization

Synthesis. The preparations of *m*′CN*p*CH$_3$ [Sm6p] (Merchant *et al.*, 1965) and *m*′Br*p*CH$_3$ [Dm6p] have previously been reported (Budakoti *et al.*, 2008; Ellsworth *et al.*, 2008; Rangarajan *et al.*, 2016; Soni & Patel, 2017; Zhang *et al.*, 2017). Ethanol (1.5 mL, 95%) and a magnetic stir bar were added to two separate Biotage microwave vials (2–5 mL); one contained 4-methylbenzaldehyde (3 mmol) and the other contained 3′-acetophenone (3 mmol). Each vial was heated gently over a hot plate until complete dissolution and then cooled to room temperature; solids may precipitate upon cooling depending on the solubility of the starting material. Once cooled, NaOH (aq) (0.4 mL, 50% by wgt) was added to a benzaldehyde–acetophenone mixture. The resulting reaction mixture was vigorously agitated with a microspatula until a slurry formed. Water (2 mL) was added to the vial and its contents were agitated. The vial was capped, centrifuged for one minute, and decanted. This trituration was repeated three times. Methanol (2 mL) was added to the vessel and sealed; the microwave-safe vials are safe at high pressures, up to 30 bar. Over a hot plate while stirring, the contents were heated until complete dissolution. Once removed from the heat, the vial was allowed to cool, and crystal growth was observed. Crystals were isolated and dried using vacuum filtration. ^{1}H NMR (400 MHz, $CDCl_3$, referenced to TMS): δ (ppm) for *m*′Br*p*CH$_3$ are 8.13 (*t*, 1H, *J* = 1.7 Hz), 7.93 (*ddd*, 1H, *J* = 7.8, 1.4, 1.0 Hz), 7.80 (*d*, 1H, *J* = 15.6 Hz), 7.70 (*ddd*, 1H, *J* = 8.0, 2.0, 1.0 Hz), 7.55 (*d*, 2H, *J* = 8.1 Hz), 7.40 (*m*, 2H), 7.23 (*d*, 2H, *J* = 8.0 Hz), 2.40 (*s*, 3H); and for *m*′CN*p*CH$_3$ are 8.28 (*t*, 1H, *J* = 1.2 Hz), 8.23 (*ddd*, 1H, *J* = 7.9, 1,7, 1.2 Hz), 7.84 (*m*, 2H), 7.64 (*t*, 1H, *J* = 7.9 Hz), 7.56 (*d*, 2H, *J* = 8.1 Hz), 7.43 (*d*, 1H, *J* = 15.6 Hz), 7.25 (*d*, 2H, *J* = 8.5 Hz), 2.41 (*s*, 3H). ^{13}C NMR (100 MHz, $CDCl_3$, referenced to solvent, 77.16 ppm): δ (ppm) for *m*′Br*p*CH$_3$ are 189.25, 145.97, 141.63, 140.29, 135.63, 132.01, 131.60, 130.32, 129.91, 128.77, 127.10, 123.07, 120.51, 21.72; and for *m*′CN*p*CH$_3$ are 188.48, 146.82, 142.01, 139.29, 135.65, 132.53, 132.20, 131.73, 129.98, 129.77, 128.87, 119.83, 118.21, 113.20, 21.74.

Crystallization. *m*′Br*p*CH$_3$ and *m*′CN*p*CH$_3$ were crystallized through slow cooling in a Dewar hemispherical low-form flask. Chalcone (20 mg), methanol (0.5 mL), and a magnetic spin vane were added to a conical Biotage microwave vial (0.5–2 mL) and sealed. The tube was placed in boiling water for 1–5 minutes until complete dissolution. While the tube was submerged, two Dewar hemispherical low-form flasks were filled with boiling water and allowed to sit. When the chalcone had nearly dissolved, the Dewar flasks were emptied, and one was placed in a Styrofoam cooler. The Biotage microwave vial was removed from boiling water and placed in the Dewar inside the cooler. The Dewar was filled with boiling water to completely submerge the microwave vial. A round silicone gasket was placed to cover the rim of this Dewar flask before inverting the second Dewar and placing it on top to create a chamber. The cooler was closed with a Styrofoam lid on a low-vibration table in a temperature-regulated room. After 24 h, the vials were removed from the Dewar and crystals were collected using vacuum filtration.

6. Refinement

Crystal data, data collection and structure refinement details are summarized in Table 3. The X-ray intensity data for each chalcone derivative was measured at 100 K on a Bruker Photon II D8 Venture diffractometer equipped with both IμS-Cu and IμS-Mo microfocus X-ray sources. The Cu *K*α (λ = 1.54178 Å) source was used for all crystallographic investigations. Data sets were corrected for Lorentz and polarization effects as well as absorption. The criterion for observed

Table 3
Experimental details.

	m′CN*p*CH$_3$	*m*′Br*p*CH$_3$
Crystal data		
Chemical formula	$C_{17}H_{13}NO$	$C_{16}H_{13}BrO$
M_r	247.28	301.17
Crystal system, space group	Monoclinic, $P2_1/c$	Triclinic, $P\overline{1}$
Temperature (K)	100	100
a, b, c (Å)	7.2986 (1), 5.8504 (1), 29.7783 (5)	5.9282 (6), 7.3614 (8), 14.6747 (16)
α, β, γ (°)	90, 94.525 (1), 90	88.532 (3), 82.199 (3), 87.457 (3)
V (Å^3)	1267.56 (4)	633.73 (12)
Z	4	2
D_x (Mg m^{-3})	1.296	1.578
Radiation type	Cu $K\alpha$	Cu $K\alpha$
μ (mm^{-1})	0.64	4.28
Crystal shape	Transparent plate	Transparent plate
Colour	Colourless	Colorless
Crystal size (mm)	0.35 × 0.21 × 0.09	0.39 × 0.25 × 0.11
Data collection		
Diffractometer	Bruker D8 Venture	Bruker D8 Venture
Absorption correction	Multi-scan (*SADABS*; Krause *et al.*, 2015)	Multi-scan (*SADABS*; Krause *et al.*, 2015)
T_{min}, T_{max}	0.676, 0.754	0.531, 0.754
No. of measured, independent and observed [$I > 2\sigma(I)$] reflections	13801, 2494, 2213	8397, 2461, 2440
R_{int}	0.028	0.023
$(\sin\theta/\lambda)_{max}$ (Å^{-1})	0.617	0.617
Refinement		
$R[F^2 > 2\sigma(F^2)]$, $wR(F^2)$, S	0.033, 0.087, 1.03	0.026, 0.065, 1.09
No. of reflections	2494	2461
No. of parameters	173	164
H-atom treatment	H-atom parameters constrained	H-atom parameters constrained
$\Delta\rho_{max}$, $\Delta\rho_{min}$ (e Å^{-3})	0.21, −0.18	0.63, −0.40

Computer programs: *APEX3* (Bruker, 2018), *SAINT* (Bruker, 2017), *SHELXT2018/2* (Sheldrick, 2015*a*), *SHELXL2018/3* (Sheldrick, 2015*b*) and *X-SEED* (Barbour, 2001).

reflections is $I > 2\sigma(I)$. Lattice parameters were determined from least-squares analysis of reflection data. Empirical absorption corrections were applied using *SADABS* (Krause *et al.*, 2015). Structures were solved by direct methods and refined by full-matrix least-squares analysis on F^2 using *X-SEED* equipped with *SHELXT* (Barbour, 2001 and Sheldrick, 2015*a*). All non-hydrogen atoms were refined anisotropically by full-matrix least-squares on F^2 using the *SHELXL* program (Sheldrick, 2015*b*). H atoms (for OH and NH) were located in a difference-Fourier synthesis and refined isotropically with independent O/N—H distances or restrained to 0.85 (2) Å. The remaining H atoms were included in idealized geometric positions with U_{iso}(H) = 1.2U_{eq}(parent atom) or 1.5U_{eq}(C-methyl).

Unit cells were visualized with *Mercury 2020.1* (Macrae *et al.*, 2020), Hirshfeld analyses were executed with *Crystal Explorer 17.5* (Turner *et al.*, 2017), while distance/angle measurements as well as *ORTEP* images were captured using *OLEX2* (Dolomanov *et al.*, 2009).

Acknowledgements

The GU co-authors thank S. Economu, B. Hendricks, A. Hinz, J. Hazen, C. Sciammas, M. Plese, T. Cherry, A. Fijalka, and C. Mozo-Olazcon for their assistance, as well as the Howard Hughes Medical Institute for supporting equipment acquisition through its Undergraduate Science Education Program. Support also came from the Gonzaga Science Research Program as well as Gonzaga's Department of Chemistry and Biochemistry.

Funding information

Funding for this research was provided by: EPSRC (grant No. EP/L015544/1 to C. L. Hall; grant No. EP/L016648/1 to V. Hamilton); European Union's Horizon 2020 Research and Innovation Programme (grant No. 736899); funding for the Bruker Photon II D8 Venture diffractometer was provided by NSF-MRI #1827313.

References

Barbour, L. J. (2001). *J. Supramol. Chem.* **1**, 189–191.
Braun, R. U., Ansorge, M. & Müller, T. J. J. (2006*a*). *Chem. Eur. J.* **12**, 9081–9094.
Braun, R. U., Müller, T. J. J. & Polborn, K. (2006*b*). Private communication (refcode NAWCEU). CCDC, Cambridge, England.
Bruker (2017). *SAINT*. Bruker AXS Inc., Madison, Wisconsin, USA.
Bruker (2018). *APEX3*. Bruker AXS Inc., Madison, Wisconsin, USA.
Budakoti, A., Bhat, A. R., Athar, F. & Azam, A. (2008). *Eur. J. Med. Chem.* **43**, 1749–1757.
Cavallo, G., Metrangolo, P., Milani, R., Pilati, T., Priimagi, A., Resnati, G. & Terraneo, G. (2016). *Chem. Rev.* **116**, 2478–2601.
Dinadayalane, T. & Leszczynski, J. (2009). *Struct. Chem.* **20**, 11–20.
Dolomanov, O. V., Bourhis, L. J., Gildea, R. J., Howard, J. A. K. & Puschmann, H. (2009). *J. Appl. Cryst.* **42**, 339–341.

Ellsworth, B. A., Meng, W., Patel, M., Girotra, R. N., Wu, G., Sher, P. M., Hagan, D. L., Obermeier, M. T., Humphreys, W. G., Robertson, J. G., Wang, A., Han, S., Waldron, T. L., Morgan, N. N., Whaley, J. M. & Washburn, W. N. (2008). *Bioorg. Med. Chem. Lett.* **18**, 4770–4773.
Frisch, M. J., Trucks, G. W., Schlegel, H. B., Scuseria, G. E., Robb, M. A., Cheeseman, J. R., Scalmani, G., Barone, V., Mennucci, B., Petersson, G. A., Nakatsuji, H., Caricato, M., Li, X., Hratchian, H. P., Izmaylov, A. F., Bloino, J., Zheng, G., Sonnenberg, J. L., Hada, M., Ehara, M., Toyota, K., Fukuda, R., Hasegawa, J., Ishida, M., Nakajima, T., Honda, Y., Kitao, O., Nakai, H., Vreven, T., Montgomery, J. A. Jr, Peralta, J. E., Ogliaro, F., Bearpark, M., Heyd, J. J., Brothers, E., Kudin, K. N., Staroverov, V. N., Kobayashi, R., Normand, J., Raghavachari, K., Rendell, A., Burant, J. C., Iyengar, S. S., Tomasi, J., Cossi, M., Rega, N., Millam, J. M., Klene, M., Knox, J. E., Cross, J. B., Bakken, V., Adamo, C., Jaramillo, J., Gomperts, R., Stratmann, R. E., Yazyev, O., Austin, A. J., Cammi, R., Pomelli, C., Ochterski, J. W., Martin, R. L., Morokuma, K., Zakrzewski, V. G., Voth, G. A., Salvador, P., Dannenberg, J. J., Dapprich, S., Daniels, A. D., Farkas, Ö., Foresman, J. B., Ortiz, J. V., Cioslowski, J. & Fox, D. J. (2009). *Gaussian 09*, Revision D. 01. Gaussian Inc., Wallingford, CT, USA.
Groom, C. R., Bruno, I. J., Lightfoot, M. P. & Ward, S. C. (2016). *Acta Cryst.* B**72**, 171–179.
Krause, L., Herbst-Irmer, R., Sheldrick, G. M. & Stalke, D. (2015). *J. Appl. Cryst.* **48**, 3–10.
Lee, S. C., Kang, N. Y., Park, S. J., Yun, S. W., Chandran, Y. & Chang, Y. T. (2012). *Chem. Commun.* **48**, 6681–6683.
Li, H., Sarojini, B. K., Raj, C. G. D., Madhu, L. N. & Yathirajan, H. S. (2008). *Acta Cryst.* E**64**, o2238.
Macrae, C. F., Sovago, I., Cottrell, S. J., Galek, P. T. A., McCabe, P., Pidcock, E., Platings, M., Shields, G. P., Stevens, J. S., Towler, M. & Wood, P. A. (2020). *J. Appl. Cryst.* **53**, 226–235.
Merchant, J. R., Mehta, J. B. & Desai, V. B. (1965). *Indian J. Chem.* **3**, 561–4.
Rangarajan, T. M., Devi, K., Verma, A. K., Singh, R. P. & Singh, R. P. (2016). *J. Fluor. Chem.* **186**, 101–110.
Rosli, M. M., Patil, P. S., Fun, H.-K., Razak, I. A. & Dharmaprakash, S. M. (2007). *Acta Cryst.* E**63**, o2501.
Sahu, N. K., Balbhadra, S. S., Choudhary, J. & Kohli, D. V. (2012). *Curr. Med. Chem.* **19**, 209–225.
Sheldrick, G. M. (2015*a*). *Acta Cryst.* A**71**, 3–8.
Sheldrick, G. M. (2015*b*). *Acta Cryst.* C**71**, 3–8.
Soni, H. I. & Patel, N. B. (2017). *Asia. J. Pharm. Clin. Res.* **10**, 209–214.
Spackman, M. A. & Jayatilaka, D. (2009). *CrystEngComm*, **11**, 19–32.
Turner, M. J., McKinnon, J. J., Wolff, S. K., Grimwood, D. J., Spackman, P. R., Jayatilaka, D. & Spackman, M. A. (2017). *CrystalExplorer17.5*. The University of Western Australia.
Wang, L., Zhang, Y., Lu, C.-R. & Zhang, D.-C. (2004). *Acta Cryst.* C**60**, o696–o698.
Wheeler, S. E. (2011). *J. Am. Chem. Soc.* **133**, 10262–10274.
Zhang, M., Xi, J., Ruzi, R., Li, N., Wu, Z., Li, W. & Zhu, C. (2017). *J. Org. Chem.* **82**, 9305–9311.
Zhuang, C., Zhang, W., Sheng, C., Zhang, W., Xing, C. & Miao, Z. (2017). *Chem. Rev.* **117**, 7762–7810.

supporting information

Acta Cryst. (2020). E**76**, 1496-1502 [https://doi.org/10.1107/S2056989020011135]

Crystal structure and Hirshfeld analysis of 3′-bromo-4-methylchalcone and 3′-cyano-4-methylchalcone

Zachary O. Battaglia, Jordan T. Kersten, Elise M. Nicol, Paloma Whitworth, Kraig A. Wheeler, Charlie L. Hall, Jason Potticary, Victoria Hamilton, Simon R. Hall, Gemma D. D'Ambruoso, Masaomi Matsumoto, Stephen D. Warren and Matthew E. Cremeens

Computing details

For both structures, data collection: *APEX3* (Bruker, 2018); cell refinement: *SAINT* (Bruker, 2017); data reduction: *SAINT* (Bruker, 2017); program(s) used to solve structure: *SHELXT2018/2* (Sheldrick, 2015a); program(s) used to refine structure: *SHELXL2018/3* (Sheldrick, 2015b); molecular graphics: *X-SEED* (Barbour, 2001); software used to prepare material for publication: *X-SEED* (Barbour, 2001).

2-[3-(4-Methylphenyl)prop-2-enoyl]benzonitrile (I)

Crystal data

$C_{17}H_{13}NO$
$M_r = 247.28$
Monoclinic, $P2_1/c$
$a = 7.2986$ (1) Å
$b = 5.8504$ (1) Å
$c = 29.7783$ (5) Å
$\beta = 94.525$ (1)°
$V = 1267.56$ (4) Å^3
$Z = 4$
$F(000) = 520$
$D_x = 1.296$ Mg m^{-3}
Cu $K\alpha$ radiation, $\lambda = 1.54178$ Å
Cell parameters from 7537 reflections
$\theta = 3.0$–$72.1°$
$\mu = 0.64$ mm^{-1}
$T = 100$ K
Transparent plate, colourless
0.35 × 0.21 × 0.09 mm

Data collection

Bruker D8 Venture diffractometer
Radiation source: Microsource IuS Incoatec 3.0
Double Bounce Multilayer Mirrors monochromator
Detector resolution: 7.9 pixels mm^{-1}
φ and ω scans
Absorption correction: multi-scan (SADABS; Krause *et al.*, 2015)
$T_{min} = 0.676$, $T_{max} = 0.754$
13801 measured reflections
2494 independent reflections
2213 reflections with $I > 2\sigma(I)$
$R_{int} = 0.028$
$\theta_{max} = 72.1°$, $\theta_{min} = 3.0°$
$h = -9\rightarrow8$
$k = -7\rightarrow7$
$l = -36\rightarrow36$

Refinement

Refinement on F^2
Least-squares matrix: full
$R[F^2 > 2\sigma(F^2)] = 0.033$
$wR(F^2) = 0.087$
$S = 1.03$
2494 reflections
173 parameters
0 restraints
Primary atom site location: structure-invariant direct methods
Hydrogen site location: inferred from neighbouring sites

H-atom parameters constrained
$w = 1/[\sigma^2(F_o^2) + (0.045P)^2 + 0.4265P]$
where $P = (F_o^2 + 2F_c^2)/3$

$(\Delta/\sigma)_{max} = 0.001$
$\Delta\rho_{max} = 0.21$ e Å^{-3}
$\Delta\rho_{min} = -0.18$ e Å^{-3}

Special details

Geometry. All esds (except the esd in the dihedral angle between two l.s. planes) are estimated using the full covariance matrix. The cell esds are taken into account individually in the estimation of esds in distances, angles and torsion angles; correlations between esds in cell parameters are only used when they are defined by crystal symmetry. An approximate (isotropic) treatment of cell esds is used for estimating esds involving l.s. planes.

Refinement. All nonhydrogen atoms were located in a single difference Fourier electron density map and refined using anisotropic displacement parameters. All C-H hydrogen atoms were placed in calculated positions with Uiso = 1.2xUeqiv of the connected C atoms (1.5xUeqiv for methyl groups).

Fractional atomic coordinates and isotropic or equivalent isotropic displacement parameters (Å²)

	x	*y*	*z*	U_{iso}*/U_{eq}
O1	0.22192 (11)	0.72690 (13)	0.47783 (2)	0.02168 (19)
N1	0.13188 (15)	0.75910 (19)	0.27529 (3)	0.0286 (2)
C1	0.21471 (14)	0.52052 (18)	0.47083 (3)	0.0165 (2)
C2	0.26906 (14)	0.35011 (18)	0.50599 (3)	0.0174 (2)
H2	0.282576	0.194303	0.497894	0.021*
C3	0.29943 (14)	0.41308 (18)	0.54913 (3)	0.0160 (2)
H3	0.282067	0.570173	0.555670	0.019*
C4	0.14995 (14)	0.43210 (18)	0.42488 (3)	0.0159 (2)
C5	0.16826 (14)	0.57332 (18)	0.38769 (3)	0.0163 (2)
H5	0.221501	0.720872	0.391577	0.020*
C6	0.10757 (14)	0.49562 (19)	0.34474 (3)	0.0171 (2)
C7	0.02732 (14)	0.27968 (19)	0.33848 (4)	0.0187 (2)
H7	−0.013000	0.227830	0.309115	0.022*
C8	0.00746 (14)	0.14251 (19)	0.37570 (4)	0.0189 (2)
H8	−0.049184	−0.003134	0.371874	0.023*
C9	0.06980 (14)	0.21624 (18)	0.41866 (4)	0.0176 (2)
H9	0.057822	0.119396	0.443864	0.021*
C10	0.35662 (14)	0.26495 (18)	0.58726 (3)	0.0152 (2)
C11	0.33577 (14)	0.34331 (19)	0.63106 (3)	0.0173 (2)
H11	0.287002	0.491628	0.635291	0.021*
C12	0.38509 (15)	0.20805 (19)	0.66834 (3)	0.0186 (2)
H12	0.366765	0.263493	0.697639	0.022*
C13	0.46133 (14)	−0.00854 (19)	0.66336 (3)	0.0173 (2)
C14	0.48597 (14)	−0.08447 (18)	0.61969 (4)	0.0171 (2)
H14	0.540026	−0.229971	0.615618	0.021*
C15	0.43333 (14)	0.04771 (18)	0.58221 (3)	0.0164 (2)
H15	0.449373	−0.009384	0.552915	0.020*
C16	0.12291 (15)	0.6427 (2)	0.30610 (4)	0.0206 (2)
C17	0.51598 (16)	−0.1542 (2)	0.70393 (4)	0.0227 (2)
H17A	0.627558	−0.091602	0.719826	0.034*
H17B	0.539551	−0.310760	0.694210	0.034*
H17C	0.416382	−0.154959	0.724164	0.034*

Atomic displacement parameters (Å²)

	U^{11}	U^{22}	U^{33}	U^{12}	U^{13}	U^{23}
O1	0.0290 (4)	0.0159 (4)	0.0197 (4)	0.0010 (3)	−0.0009 (3)	−0.0006 (3)
N1	0.0352 (6)	0.0302 (6)	0.0197 (5)	−0.0055 (5)	−0.0016 (4)	0.0035 (4)
C1	0.0144 (5)	0.0176 (5)	0.0178 (5)	0.0007 (4)	0.0024 (4)	−0.0003 (4)
C2	0.0185 (5)	0.0157 (5)	0.0179 (5)	0.0019 (4)	0.0012 (4)	0.0001 (4)
C3	0.0137 (5)	0.0149 (5)	0.0196 (5)	−0.0004 (4)	0.0019 (4)	−0.0003 (4)
C4	0.0139 (5)	0.0163 (5)	0.0174 (5)	0.0035 (4)	0.0011 (4)	0.0000 (4)
C5	0.0146 (5)	0.0149 (5)	0.0192 (5)	0.0016 (4)	0.0007 (4)	0.0000 (4)
C6	0.0155 (5)	0.0186 (5)	0.0172 (5)	0.0031 (4)	0.0010 (4)	0.0015 (4)
C7	0.0171 (5)	0.0205 (5)	0.0182 (5)	0.0033 (4)	−0.0013 (4)	−0.0039 (4)
C8	0.0168 (5)	0.0152 (5)	0.0244 (5)	0.0006 (4)	−0.0003 (4)	−0.0013 (4)
C9	0.0164 (5)	0.0162 (5)	0.0202 (5)	0.0022 (4)	0.0014 (4)	0.0023 (4)
C10	0.0128 (5)	0.0164 (5)	0.0161 (5)	−0.0023 (4)	0.0005 (4)	−0.0005 (4)
C11	0.0167 (5)	0.0156 (5)	0.0195 (5)	−0.0010 (4)	0.0018 (4)	−0.0023 (4)
C12	0.0205 (5)	0.0209 (5)	0.0146 (5)	−0.0024 (4)	0.0017 (4)	−0.0034 (4)
C13	0.0160 (5)	0.0193 (5)	0.0164 (5)	−0.0036 (4)	−0.0004 (4)	0.0015 (4)
C14	0.0162 (5)	0.0148 (5)	0.0205 (5)	−0.0001 (4)	0.0020 (4)	−0.0004 (4)
C15	0.0158 (5)	0.0185 (5)	0.0150 (5)	−0.0010 (4)	0.0021 (4)	−0.0014 (4)
C16	0.0210 (5)	0.0222 (6)	0.0182 (5)	−0.0011 (4)	−0.0013 (4)	−0.0024 (5)
C17	0.0260 (6)	0.0230 (6)	0.0188 (5)	−0.0008 (5)	−0.0001 (4)	0.0039 (4)

Geometric parameters (Å, º)

O1—C1	1.2257 (13)	C8—H8	0.9500
N1—C16	1.1487 (15)	C9—H9	0.9500
C1—C2	1.4771 (15)	C10—C15	1.4017 (15)
C1—C4	1.5038 (14)	C10—C11	1.4021 (14)
C2—C3	1.3380 (15)	C11—C12	1.3875 (15)
C2—H2	0.9500	C11—H11	0.9500
C3—C10	1.4629 (14)	C12—C13	1.3965 (16)
C3—H3	0.9500	C12—H12	0.9500
C4—C5	1.3966 (15)	C13—C14	1.3992 (15)
C4—C9	1.3980 (15)	C13—C17	1.5062 (14)
C5—C6	1.3961 (14)	C14—C15	1.3869 (15)
C5—H5	0.9500	C14—H14	0.9500
C6—C7	1.3988 (16)	C15—H15	0.9500
C6—C16	1.4482 (15)	C17—H17A	0.9800
C7—C8	1.3852 (16)	C17—H17B	0.9800
C7—H7	0.9500	C17—H17C	0.9800
C8—C9	1.3920 (15)		
O1—C1—C2	122.61 (10)	C4—C9—H9	119.8
O1—C1—C4	119.98 (9)	C15—C10—C11	118.03 (9)
C2—C1—C4	117.41 (9)	C15—C10—C3	123.08 (9)
C3—C2—C1	120.63 (10)	C11—C10—C3	118.89 (10)
C3—C2—H2	119.7	C12—C11—C10	121.16 (10)

C1—C2—H2	119.7	C12—C11—H11	119.4
C2—C3—C10	126.70 (10)	C10—C11—H11	119.4
C2—C3—H3	116.6	C11—C12—C13	120.86 (10)
C10—C3—H3	116.6	C11—C12—H12	119.6
C5—C4—C9	119.63 (10)	C13—C12—H12	119.6
C5—C4—C1	118.38 (10)	C12—C13—C14	117.92 (9)
C9—C4—C1	121.98 (9)	C12—C13—C17	120.70 (9)
C6—C5—C4	119.38 (10)	C14—C13—C17	121.37 (10)
C6—C5—H5	120.3	C15—C14—C13	121.54 (10)
C4—C5—H5	120.3	C15—C14—H14	119.2
C5—C6—C7	121.03 (10)	C13—C14—H14	119.2
C5—C6—C16	119.71 (10)	C14—C15—C10	120.45 (10)
C7—C6—C16	119.24 (9)	C14—C15—H15	119.8
C8—C7—C6	119.06 (10)	C10—C15—H15	119.8
C8—C7—H7	120.5	N1—C16—C6	178.83 (12)
C6—C7—H7	120.5	C13—C17—H17A	109.5
C7—C8—C9	120.57 (10)	C13—C17—H17B	109.5
C7—C8—H8	119.7	H17A—C17—H17B	109.5
C9—C8—H8	119.7	C13—C17—H17C	109.5
C8—C9—C4	120.32 (10)	H17A—C17—H17C	109.5
C8—C9—H9	119.8	H17B—C17—H17C	109.5

O1—C1—C2—C3	11.34 (17)	C5—C4—C9—C8	−0.38 (15)
C4—C1—C2—C3	−169.15 (10)	C1—C4—C9—C8	178.43 (9)
C1—C2—C3—C10	−178.91 (9)	C2—C3—C10—C15	17.24 (17)
O1—C1—C4—C5	24.95 (15)	C2—C3—C10—C11	−163.34 (10)
C2—C1—C4—C5	−154.58 (10)	C15—C10—C11—C12	−1.61 (15)
O1—C1—C4—C9	−153.88 (10)	C3—C10—C11—C12	178.95 (9)
C2—C1—C4—C9	26.59 (14)	C10—C11—C12—C13	1.57 (16)
C9—C4—C5—C6	−0.58 (15)	C11—C12—C13—C14	−0.10 (16)
C1—C4—C5—C6	−179.43 (9)	C11—C12—C13—C17	179.55 (10)
C4—C5—C6—C7	0.60 (16)	C12—C13—C14—C15	−1.32 (16)
C4—C5—C6—C16	178.85 (9)	C17—C13—C14—C15	179.03 (10)
C5—C6—C7—C8	0.34 (16)	C13—C14—C15—C10	1.28 (16)
C16—C6—C7—C8	−177.92 (10)	C11—C10—C15—C14	0.19 (15)
C6—C7—C8—C9	−1.30 (16)	C3—C10—C15—C14	179.62 (10)
C7—C8—C9—C4	1.34 (16)		

1-(2-Bromophenyl)-3-(4-methylphenyl)prop-2-en-1-one (II)

Crystal data

$C_{16}H_{13}BrO$
$M_r = 301.17$
Triclinic, $P\overline{1}$
$a = 5.9282$ (6) Å
$b = 7.3614$ (8) Å
$c = 14.6747$ (16) Å
$\alpha = 88.532$ (3)°
$\beta = 82.199$ (3)°
$\gamma = 87.457$ (3)°
$V = 633.73$ (12) Å^3
$Z = 2$
$F(000) = 304$
$D_x = 1.578$ Mg m^{-3}
Cu $K\alpha$ radiation, $\lambda = 1.54178$ Å
Cell parameters from 1318 reflections
$\theta = 6.0$–71.7°

μ = 4.28 mm^{-1}
T = 100 K

Transparent plate, colorless
0.39 × 0.25 × 0.11 mm

Data collection

Bruker D8 Venture diffractometer
Radiation source: Microsource IuS Incoatec 3.0
Double Bounce Multilayer Mirrors monochromator
Detector resolution: 7.9 pixels mm^{-1}
φ and ω scans
Absorption correction: multi-scan (SADABS; Krause *et al.*, 2015)

T_{min} = 0.531, T_{max} = 0.754
8397 measured reflections
2461 independent reflections
2440 reflections with $I > 2\sigma(I)$
R_{int} = 0.023
θ_{max} = 72.2°, θ_{min} = 3.0°
h = −6→7
k = −9→9
l = −18→18

Refinement

Refinement on F^2
Least-squares matrix: full
$R[F^2 > 2\sigma(F^2)]$ = 0.026
$wR(F^2)$ = 0.065
S = 1.09
2461 reflections
164 parameters
0 restraints

Primary atom site location: structure-invariant direct methods
Hydrogen site location: inferred from neighbouring sites
H-atom parameters constrained
$w = 1/[\sigma^2(F_o^2) + (0.0313P)^2 + 0.5783P]$ where $P = (F_o^2 + 2F_c^2)/3$
$(\Delta/\sigma)_{max}$ = 0.001
$\Delta\rho_{max}$ = 0.63 e Å^{-3}
$\Delta\rho_{min}$ = −0.40 e Å^{-3}

Special details

Geometry. All esds (except the esd in the dihedral angle between two l.s. planes) are estimated using the full covariance matrix. The cell esds are taken into account individually in the estimation of esds in distances, angles and torsion angles; correlations between esds in cell parameters are only used when they are defined by crystal symmetry. An approximate (isotropic) treatment of cell esds is used for estimating esds involving l.s. planes.

Refinement. All nonhydrogen atoms were located in a single difference Fourier electron density map and refined using anisotropic displacement parameters. All C-H hydrogen atoms were placed in calculated positions with Uiso = 1.2xUeqiv of the connected C atoms (1.5xUeqiv for methyl groups).

Fractional atomic coordinates and isotropic or equivalent isotropic displacement parameters (Å²)

	x	*y*	*z*	U_{iso}*/U_{eq}
Br1	0.80035 (3)	0.89029 (3)	0.08237 (2)	0.02192 (9)
O1	0.7329 (2)	0.7890 (2)	0.45698 (9)	0.0223 (3)
C1	0.5354 (3)	0.7917 (2)	0.44225 (13)	0.0170 (4)
C2	0.3466 (3)	0.7319 (3)	0.51279 (13)	0.0192 (4)
H2	0.199245	0.718770	0.495759	0.023*
C3	0.3817 (3)	0.6965 (2)	0.59951 (13)	0.0186 (4)
H3	0.530796	0.713033	0.613915	0.022*
C4	0.4726 (3)	0.8590 (2)	0.35130 (13)	0.0155 (3)
C5	0.6366 (3)	0.8439 (2)	0.27330 (13)	0.0161 (3)
H5	0.783980	0.791310	0.277957	0.019*
C6	0.5803 (3)	0.9069 (2)	0.18959 (12)	0.0167 (3)
C7	0.3658 (3)	0.9867 (2)	0.18070 (13)	0.0189 (4)
H7	0.330243	1.029208	0.122449	0.023*
C8	0.2067 (3)	1.0024 (2)	0.25840 (14)	0.0192 (4)

H8	0.061052	1.058189	0.253582	0.023*
C9	0.2567 (3)	0.9378 (2)	0.34359 (13)	0.0175 (4)
H9	0.144730	0.947060	0.396286	0.021*
C10	0.2121 (3)	0.6346 (2)	0.67464 (13)	0.0180 (4)
C11	0.2535 (3)	0.6525 (2)	0.76554 (14)	0.0197 (4)
H11	0.393474	0.699115	0.777189	0.024*
C12	0.0940 (3)	0.6036 (3)	0.83870 (13)	0.0204 (4)
H12	0.124142	0.620360	0.899810	0.025*
C13	−0.1104 (3)	0.5301 (2)	0.82409 (13)	0.0188 (4)
C14	−0.1492 (3)	0.5068 (2)	0.73322 (13)	0.0191 (4)
H14	−0.285712	0.453991	0.721786	0.023*
C15	0.0076 (3)	0.5594 (3)	0.65972 (13)	0.0195 (4)
H15	−0.023652	0.544247	0.598635	0.023*
C16	−0.2846 (4)	0.4761 (3)	0.90371 (14)	0.0243 (4)
H16A	−0.238535	0.357702	0.928866	0.036*
H16B	−0.433393	0.467934	0.882360	0.036*
H16C	−0.295102	0.567581	0.951623	0.036*

Atomic displacement parameters (Å²)

	U^{11}	U^{22}	U^{33}	U^{12}	U^{13}	U^{23}
Br1	0.02062 (13)	0.02741 (13)	0.01669 (12)	−0.00258 (8)	0.00161 (8)	0.00044 (8)
O1	0.0152 (7)	0.0321 (7)	0.0196 (7)	−0.0023 (5)	−0.0024 (5)	0.0007 (5)
C1	0.0174 (9)	0.0142 (8)	0.0194 (9)	−0.0018 (7)	−0.0019 (7)	−0.0021 (6)
C2	0.0175 (9)	0.0191 (9)	0.0206 (9)	−0.0019 (7)	−0.0008 (7)	−0.0013 (7)
C3	0.0176 (9)	0.0142 (8)	0.0237 (9)	0.0005 (7)	−0.0015 (7)	−0.0026 (7)
C4	0.0150 (8)	0.0131 (8)	0.0188 (9)	−0.0030 (6)	−0.0025 (7)	−0.0012 (6)
C5	0.0136 (8)	0.0143 (8)	0.0205 (9)	−0.0026 (6)	−0.0024 (7)	−0.0016 (7)
C6	0.0163 (9)	0.0167 (8)	0.0168 (8)	−0.0043 (7)	0.0005 (7)	−0.0012 (6)
C7	0.0198 (9)	0.0174 (8)	0.0208 (9)	−0.0042 (7)	−0.0070 (7)	0.0020 (7)
C8	0.0140 (9)	0.0167 (8)	0.0275 (10)	−0.0003 (7)	−0.0048 (7)	−0.0008 (7)
C9	0.0147 (9)	0.0157 (8)	0.0215 (9)	−0.0018 (7)	0.0001 (7)	−0.0021 (7)
C10	0.0183 (9)	0.0148 (8)	0.0209 (9)	0.0002 (7)	−0.0026 (7)	0.0011 (7)
C11	0.0196 (9)	0.0155 (8)	0.0259 (10)	−0.0007 (7)	−0.0099 (8)	0.0010 (7)
C12	0.0245 (10)	0.0175 (9)	0.0207 (9)	0.0020 (7)	−0.0092 (8)	0.0001 (7)
C13	0.0206 (9)	0.0142 (8)	0.0218 (9)	0.0030 (7)	−0.0045 (7)	0.0000 (7)
C14	0.0187 (9)	0.0167 (8)	0.0230 (9)	−0.0025 (7)	−0.0058 (7)	−0.0003 (7)
C15	0.0217 (10)	0.0189 (9)	0.0189 (9)	−0.0027 (7)	−0.0054 (7)	−0.0012 (7)
C16	0.0244 (10)	0.0272 (10)	0.0211 (9)	0.0001 (8)	−0.0027 (8)	−0.0006 (8)

Geometric parameters (Å, º)

Br1—C6	1.9053 (18)	C8—H8	0.9500
O1—C1	1.219 (2)	C9—H9	0.9500
C1—C2	1.491 (3)	C10—C11	1.399 (3)
C1—C4	1.500 (3)	C10—C15	1.401 (3)
C2—C3	1.334 (3)	C11—C12	1.382 (3)
C2—H2	0.9500	C11—H11	0.9500

C3—C10	1.465 (3)	C12—C13	1.393 (3)
C3—H3	0.9500	C12—H12	0.9500
C4—C9	1.399 (3)	C13—C14	1.400 (3)
C4—C5	1.401 (3)	C13—C16	1.508 (3)
C5—C6	1.380 (3)	C14—C15	1.384 (3)
C5—H5	0.9500	C14—H14	0.9500
C6—C7	1.398 (3)	C15—H15	0.9500
C7—C8	1.382 (3)	C16—H16A	0.9800
C7—H7	0.9500	C16—H16B	0.9800
C8—C9	1.391 (3)	C16—H16C	0.9800

O1—C1—C2	122.32 (17)	C4—C9—H9	120.2
O1—C1—C4	120.48 (17)	C11—C10—C15	118.05 (18)
C2—C1—C4	117.20 (16)	C11—C10—C3	119.08 (17)
C3—C2—C1	120.92 (17)	C15—C10—C3	122.87 (17)
C3—C2—H2	119.5	C12—C11—C10	121.11 (18)
C1—C2—H2	119.5	C12—C11—H11	119.4
C2—C3—C10	126.21 (18)	C10—C11—H11	119.4
C2—C3—H3	116.9	C11—C12—C13	120.94 (18)
C10—C3—H3	116.9	C11—C12—H12	119.5
C9—C4—C5	120.03 (17)	C13—C12—H12	119.5
C9—C4—C1	121.39 (17)	C12—C13—C14	118.08 (18)
C5—C4—C1	118.57 (16)	C12—C13—C16	121.12 (18)
C6—C5—C4	118.80 (17)	C14—C13—C16	120.80 (18)
C6—C5—H5	120.6	C15—C14—C13	121.21 (18)
C4—C5—H5	120.6	C15—C14—H14	119.4
C5—C6—C7	121.94 (17)	C13—C14—H14	119.4
C5—C6—Br1	119.84 (14)	C14—C15—C10	120.57 (18)
C7—C6—Br1	118.21 (14)	C14—C15—H15	119.7
C8—C7—C6	118.60 (17)	C10—C15—H15	119.7
C8—C7—H7	120.7	C13—C16—H16A	109.5
C6—C7—H7	120.7	C13—C16—H16B	109.5
C7—C8—C9	120.93 (17)	H16A—C16—H16B	109.5
C7—C8—H8	119.5	C13—C16—H16C	109.5
C9—C8—H8	119.5	H16A—C16—H16C	109.5
C8—C9—C4	119.69 (17)	H16B—C16—H16C	109.5
C8—C9—H9	120.2		

O1—C1—C2—C3	9.4 (3)	C5—C4—C9—C8	−0.6 (3)
C4—C1—C2—C3	−169.73 (17)	C1—C4—C9—C8	178.53 (16)
C1—C2—C3—C10	−179.08 (17)	C2—C3—C10—C11	−161.99 (18)
O1—C1—C4—C9	−151.81 (18)	C2—C3—C10—C15	17.3 (3)
C2—C1—C4—C9	27.3 (2)	C15—C10—C11—C12	−2.3 (3)
O1—C1—C4—C5	27.4 (3)	C3—C10—C11—C12	177.07 (16)
C2—C1—C4—C5	−153.51 (16)	C10—C11—C12—C13	1.8 (3)
C9—C4—C5—C6	−0.4 (3)	C11—C12—C13—C14	0.2 (3)
C1—C4—C5—C6	−179.54 (16)	C11—C12—C13—C16	179.84 (17)
C4—C5—C6—C7	0.7 (3)	C12—C13—C14—C15	−1.6 (3)

C4—C5—C6—Br1	179.46 (13)	C16—C13—C14—C15	178.69 (17)
C5—C6—C7—C8	0.0 (3)	C13—C14—C15—C10	1.1 (3)
Br1—C6—C7—C8	−178.79 (13)	C11—C10—C15—C14	0.8 (3)
C6—C7—C8—C9	−1.0 (3)	C3—C10—C15—C14	−178.51 (17)
C7—C8—C9—C4	1.3 (3)		